Structural and Functional Characterization of Human SGT and Its Interaction with Vpu of the Human Immunodeficiency Virus Type 1[†,‡]

Sujit Dutta and Yee-Joo Tan*

Collaborative Antiviral Research Group, Cancer and Developmental Cell Biology Division, Institute of Molecular and Cell Biology, Agency for Science, Technology and Research, 61 Biopolis Drive, Singapore 138673

Received April 29, 2008; Revised Manuscript Received July 30, 2008

ABSTRACT: The small glutamine-rich tetratricopeptide repeat protein (SGT) belongs to a family of cochaperones that interacts with both Hsp70 and Hsp90 via the so-called TPR domain. Here, we present the crystal structure of the TPR domain of human SGT (SGT-TPR), which shows that it contains typical features found in the structures of other TPR domains. Previous studies show that full-length SGT can bind to both Vpu and Gag of human immunodeficiency virus type 1 (HIV-1) and the overexpression of SGT in cells reduces the efficiency of HIV-1 particle release. We show that SGT-TPR can bind Vpu and reduce the amount of HIV-1 p24, which is the viral capsid, secreted from cells transfected with the HIV-1 proviral construct, albeit at a lower efficiency than full-length SGT. This indicates that the TPR domain of SGT is sufficient for the inhibition of HIV-1 particle release but the N- and/or C-terminus also have some contributions. The SGT binding site in Vpu was also identified by using peptide array and confirmed by GST pull-down assay.

The rat small glutamine-rich tetratricopeptide repeat protein (SGT)[1] was identified as a binding partner of the nonstructural protein of parvovirus H-1 (*1*). Independent studies also showed that human SGT (hSGT, also referred to as viral U-binding protein (UBP)) interacts with the human immunodeficiency virus type 1 (HIV-1) viral-encoded protein U (Vpu) and the viral core protein precursor Gag (also known as $Pr55^{gag}$) (*2*). Vpu is a 16 kDa type I integral membrane phosphoprotein that forms oligomeric structures *in vivo* and *in vitro* (*3, 4*). Vpu facilitates the degradation of CD4 receptor in the endoplasmic reticulum of infected cells (*5, 6*) and enhances release of virus particles from the plasma membrane (*4, 7*). The precursor Gag polyprotein drives the assembly and budding of HIV-1, and during virus maturation, it is cleaved to produce mature Gag proteins like the structural proteins matrix, capsid, and nucleocapsid (*8, 9*).

Overexpression of hSGT in cells transfected with a HIV-1 proviral construct has been shown to reduce the efficiency of viral particle release (*2*). Furthermore, Vpu can affect the cellular localization of both hSGT and Gag (*10*). However, much remains to be learned about the mechanism by which hSGT influences HIV-1 particle release. SGT consists of three structural units: an N-terminal self-association domain, a tetratricopeptide repeat (TPR) domain, and a C-terminal glutamine-rich domain (Figure 1A) (*1, 2, 11*). Both the N- and C-terminal domains lack significant homology to any known proteins. The centrally located TPR domain consists of three TPR motifs arranged in tandem. Each TPR motif consists of 34 amino acids and is arranged in tandem repeats of 3 to >16 (*12*−*14*). Besides its ability to bind to viral proteins, SGT has also been shown to be involved in a number of biological processes that include apoptosis, cell division, and intracellular cell transport (*15*−*19*). As TPR domains are known to mediate protein−protein interactions, it is not surprising that the TPR domain of SGT is involved in the interaction with a number of proteins such as the heat shock proteins Hsp70 and Hsp90 (*11, 20, 21*), cysteine string protein (*22*), growth hormone receptor (*23*), and androgen receptor (*15*). In addition, biochemical studies suggest that SGT is a cochaperone as it has a negative effect on the *in vitro* ATPase and refolding activity of Hsp70 (*24*). It has also been shown to be part of a trimeric protein complex that functions as an ATP-dependent chaperone (*22*). However, it is not known if the TPR domain of hSGT is important for its involvement in HIV-1 replication.

In order to gain insights into the mechanism of interaction between hSGT and Vpu, we have determined the crystal structure of the central domain of hSGT (residues 85−210). Using GST pull-down assays, we also showed that this domain is sufficient for the interaction with Vpu. Overexpression of this domain of hSGT also reduces the amount of HIV-1 p24, which is the viral capsid, secreted from cells transfected with the HIV-1 proviral construct significantly, albeit at a lower efficiency than the full-length protein. Furthermore, we have identified the hSGT binding site in Vpu.

[†] This work was supported by grants from the Agency for Science, Technology and Research (ASTAR), Singapore.

[‡] The structure of the TPR domain of SGT has been deposited in the Protein Data Bank under ID code 2VYI.

* To whom correspondence should be addressed. E-mail: mcbtanyj@imcb.a-star.edu.sg. Tel: (65)65869625. Fax: (65)67791117.

[1] Abbreviations: SGT, small glutamine-rich tetratricopeptide repeat protein; TPR, tetratricopeptide repeat; HIV-1, human immunodeficiency virus type 1; Vpu, viral-encoded protein U; GST, glutathione *S*-transferease; rmsd, root mean square deviation.

10.1021/bi800758a CCC: $40.75
Published on Web 08/30/2008

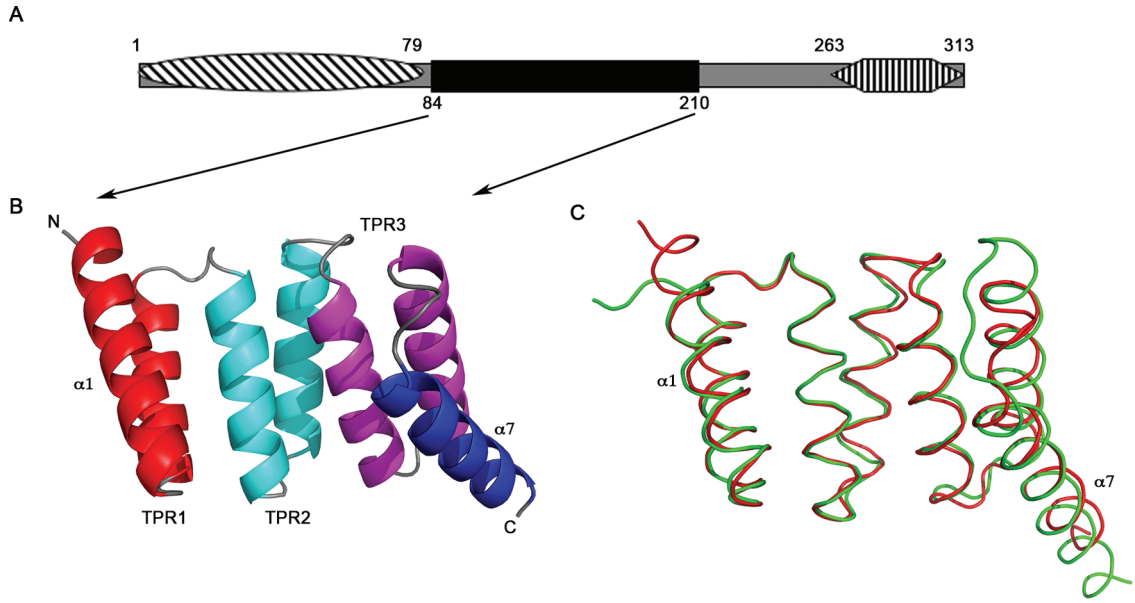

FIGURE 1: Structural features of the TPR domain of hSGT. (A) hSGT contains three functional domains: an N-terminal dimerization domain, a centrally located TPR domain, and a C-terminal glutamine-rich domain. The numbers represent the position of the amino acid residues in hSGT. (B) A ribbon representation of the structure shows three TPR motifs (red, cyan, and purple) and an additional seventh helix (blue). N- and C-termini are labeled as are the first and last helix (α1 and α7). (C) Superimposition of the TPR domains of hSGT (red) and CHIP (green). Despite sharing only 27% amino acid identity, the main chain atoms of these two TPR domains superimposed with a rmsd of only 0.94 Å. All structural figures were generated with PyMOL (http://pymol.sourceforge.net/).

EXPERIMENTAL PROCEDURES

Expression and Purification. Bioinformational analysis identified residues 85−210 of hSGT as the boundary of the TPR domain (*25*). This fragment of hSGT was expressed as a glutathione *S*-transferase (GST) (pGEX6p1; GE Healthcare) fusion protein. GST-SGT-TPR was expressed in *Escherichia coli* BL21(DE3) (Novagen). Cultures were grown at 37 °C in Luria−Bertani (LB) medium and on reaching an OD_{600} of 0.8, cells were cooled to 30 °C and induced with isopropyl β-D-1-thiogalactopyranoside (IPTG) to a final concentration of 0.2 mM. After an incubation period of 4 h, cells were harvested. Bacterial pellets were resuspended in lysis buffer (50 mM Tris-HCl (pH 7.4), 300 mM NaCl, and 2 mM DTT) supplemented with Complete protease inhibitor (Roche). For purification, cells were subjected to sonication. The lysate was cleared by centrifugation and supernatant loaded onto a 5 mL glutathione−Sepharose column (GE Healthcare) preequilibrated with lysis buffer. The column was washed to remove unbound material. Removal of the GST tag from the N-terminus of SGT-TPR was achieved by proteolytic cleavage using recombinant 3C protease (GE Healthcare). Cleaved protein was further purified by size-exclusion chromatography using a Superdex S75 column (GE Healthcare) preequilibrated in 10 mM Tris-HCl (pH 7.4), 50 mM NaCl, and 2 mM DTT. Purified SGT-TPR was concentrated to 35 mg/mL using Amicon Ultra (5 kDa cutoff; Millipore).

Crystallization and Data Collection. Crystals of recombinant SGT-TPR (35 mg/mL) were obtained at 15 °C using the sitting-drop vapor diffusion method from 1:1 μL of protein and precipitant containing 4 M sodium formate. Crystals were transferred to a reservoir solution containing 6 M sodium formate before flash freezing in liquid nitrogen.

X-ray diffraction data from a single crystal of SGT-TPR was collected at the European Synchrotron Radiation Facility (Grenoble, France) on beamline ID 14-1. Raw data were integrated and scaled using the HKL2000 program suite (*26*) (Table 1).

Table 1: Data Collection and Refinement Statistics

Data Collection	
wavelength (Å)	0.95
resolution (Å)[a]	30−2.4 (2.49−2.4)
space group	$P2_12_12$
unit cell parameters (Å; deg)	$a = 67.82$, $b = 81.93$, $c = 55.92$; $\alpha = \beta = \gamma = 90$
observed reflections[a]	61085 (5856)
unique reflections[a]	12726 (1246)
completeness (%)[a]	100 (99.0)
$I/\sigma(I)$[a]	19.2 (6.8)
R_{merge} (%)[a]	6.7 (21.5)
multiplicity[a]	4.8 (4.7)
Refinement Statistics	
R (%)	19
R_{free} (%)	25
rmsd, bond lengths (Å)	0.005
rmsd, bond angles (deg)	1.0
Model Quality (Ramachandran Plot)[b]	
residues in most favored regions (%)	91.6
residues in additional allowed regions (%)	8.4
residues in generously allowed and disallowed regions (%)	0

[a] Values in parentheses indicate values in the highest resolution shell. [b] Values from PROCHECK (*31*).

Structure Determination and Refinement. The structure of SGT-TPR was determined by the molecular replacement method, employing the TPR domain of protein phosphatase 5 (*27*) as the search model, with the program Molrep from the CCP4 suite (*28*). The model was refined with CNS (*29*), and multiple rounds of manual fitting with the program O (*30*) using $2F_o - F_c$ and $F_o - F_c$ electron density maps. The refined model consists of 190 water molecules, with a final R and R_{free} of 19.0% and 25%, respectively. There are two molecules in the asymmetric unit, termed A and B, with 128 and 123 residues, respectively. The stereochemistry of

SGT-TPR was checked with PROCHECK (*31*).The refinement statistics are summarized in Table 1.

GST Pull-Down Assay. GST pull-down assay was performed in a similar manner to that described in Callahan et al. (*2*). Briefly, the Vpu gene was amplified from pNL4-3. Luc.R-E- (*32, 33*) and cloned into a mammalian expression vector pXJ3′HA (T. Leung, Institute of Molecular and Cell Biology, Singapore, personal communication), which allows protein expression via the T7 promoter. Then, ^{35}S-labeled Vpu protein was expressed using the rabbit reticulocyte lysate *in vitro* transcription−translation system (Promega) according to the manufacturer's instruction. Approximately 30 μg of GST and GST fusion proteins were captured on glutathione−Sepharose beads, washed with Vpu-binding buffer (20 mM Tris-HCl (pH 7.9), 100 mM NaCl, 1 mM EDTA, 5% glycerol, 0.02% NP40, 0.02% BSA), and incubated with the ^{35}S-labeled Vpu protein for 2 h at 4 °C followed by 2 h at room temperature. Then the beads were washed three times with Vpu-binding buffer, and the bound proteins were eluted by boiling in Laemmli's SDS buffer for 10 min and subjected to electrophoresis on a 15% SDS−polyacrylamide gel, which was then fixed and autoradiographed.

GST-Vpu (residues 27−45) was also expressed and purified using the same method described above for GST-SGT-TPR. GST pull-down assay was then performed in the same manner using ^{35}S-labeled SGT protein produced using pXJ40flag-SGT and an *in vitro* transcription−translation system (Promega).

HIV-1 p24 Capsid Release Assay and Western Blot Analysis. The effects of SGT on HIV-1 particle release were examined by cotransfection of pXJ40flag-SGT or pXJ40flag-SGT-TPR and the HIV-1 proviral construct, pNL4-3. Luc.R-E- (*32, 33*). The plasmids pXJ40flag-SGT and pXJ40flag-SGT-TPR were constructed as previously described (*34*). Briefly, 293T cells were plated onto 6 cm dishes and allowed to attach overnight. Then, 1 μg of pNL4-3.Luc.R-E- and 2 μg of pXJ40flag vector, pXJ40flag-SGT, or pXJ40flag-SGT-TPR were cotransfected using Lipofectamine 2000 reagent (Invitrogen) according to the manufacturer's instruction. Fresh DMEM medium containing 10% FBS was added after 6 h, and the culture supernatant was collected at 48 and 72 h posttransfection. Levels of HIV-1 p24 in 1:100 dilution of each of the culture supernatant samples were quantified by use of the Alliance HIV-1 p24 antigen ELISA kit (PerkinElmer). The cells were subsequently harvested for Western blot analysis. Western blot analysis was performed as previously described (*35*), and the primary antibodies (anti-flag polyclonal and anti-actin monoclonal antibodies) were purchased from Sigma.

Mapping of the SGT-TPR Binding Motif on Vpu via Peptide Array. Overlapping peptides spanning the entire sequence of Vpu (81 amino acids) were designed so that each peptide fragment consisted of sequential 15 amino acids with an overlap of 10 amino acids between each peptide. Peptides were synthesized by JPT Petpide Technologies Gmbh (Berlin, Germany) and immobilized on a cellulose membrane. The membrane was prepared according to the manufacturer's instruction. The spot array membrane was rinsed in methanol for 5 min followed by four washes in TBS-T (50 mM Tris-HCl (pH 8.0), 137 mM NaCl, 2.7 mM KCl, 0.05% TWEEN 20) for 20 min. The membrane was subsequently incubated overnight in blocking buffer (0.1% bovine serum albumin, TBS-T) at 4 °C. GST-SGT-TPR (0.1 μg/mL) was added to the blocking buffer, and the mixture was incubated with the membrane for 2 h at room temperature. After extensive washes with TBS-T buffer to remove unbound protein, the membrane was incubated with mouse monoclonal GST antibody (Santa Cruz Biotechnology) for 2 h. The wash process was repeated, and the membrane was incubated with goat anti-mouse IgG conjugated with horseradish peroxidase (Pierce). The membrane was developed with the SuperSignal West Pico chemiluminescent substrate (Pierce) for 3 min and exposed to photographic film (GE-Healthcare). The membrane was stripped according to the manufacturer's instruction and the experiment repeated with either GST-SGT or GST.

RESULTS

Structural Determination and Overall Architecture. To aid purification, the central domain of hSGT (residues 84−210) was expressed as a N-terminal glutathione *S*-transferease fusion. The fusion was removed with the 3C protease, but five amino acids (GPLGS) remained fused to the N-terminus of the central domain of hSGT. This domain crystallized in space group $P2_12_12$. The structure was solved by molecular replacement using the structure of the TPR domain of protein phosphatase 5 (*27*) and refined to the crystallographic *R*-factor of 0.19 (R_{free} 0.25). Two molecules were identified in the asymmetric unit. Due to lack of density, residues 83−85 in the first molecule and residues 80−85 and 209−210 in the second molecule were not observed. The refinement statistics are shown in Table 1.

The TPR domain of hSGT consists of three TPR motifs (TPR 1−3) arranged in tandem and shows typical features found in the structures of other TPR domains (*27, 36*−*38*) (Figure 1B). Each TPR motif consists of a pair of α-helices arranged in an antiparallel fashion and is structurally almost identical; main chain atoms of TPR1 superimpose with TPR2 and TPR3 with a root mean square deviation (rmsd) of 0.45 and 0.41 Å, respectively. At the C-terminus of TPR3, there is an additional helix, which is the equivalent of the "capping and/or solubility" helix (termed as the C-helix) that packs against the second helix in TPR3. The C-helix is present in almost all of the TPR structures solved to date and appears to be an integral part of the TPR domain (*13*). We shall term this domain of hSGT (residues 85−210), i.e., TPR1-3 and C-helix, as SGT-TPR in this paper.

Structural comparisons with other TPR domain structures reveal the conservation of the overall structure despite low sequence identity. The highest degree of similarity is observed with the TPR domain of CHIP (C-terminal of Hsp70 interaction protein) (PDB code 2C2V) (*38*). The main chain atoms of the TPR domain of CHIP superimpose with SGT-TPR with an rmsd of 0.94 Å despite 27% sequence homology. In comparison with CHIP-TPR, the first helix of TPR1 (α1) of SGT-TPR is elongated. Furthermore, the loop connecting TPR3 to the C-helix (α7) is shorter (Figure 1C and 5A).

The TPR Domain of SGT Is Sufficient for the Binding of Vpu. In vitro GST pull-down assay was previously used to demonstrate the interaction between SGT and Vpu (*2*). Here, the assay was repeated to determine if the TPR domain of SGT alone is sufficient for the binding of Vpu. As shown in

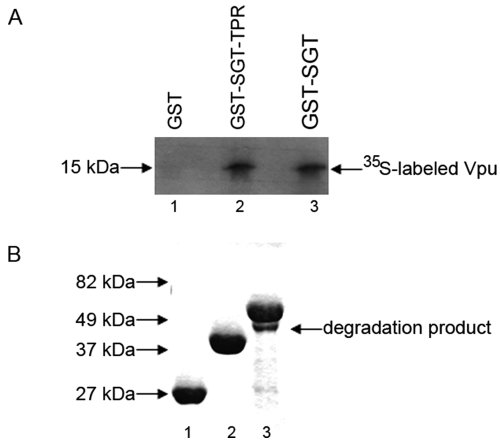

FIGURE 2: Binding between SGT and Vpu determined by GST pull-down assay. (A) GST (lane 1) and GST fusion proteins (SGT-TPR (lane 2) and full-length SGT (lane 3)) were expressed in *E. coli* and affinity purified with glutathione−Sepharose beads. GST pull-down assays were then carried out by mixing the bacterially expressed proteins bound to glutathione−Sepharose beads with *in vitro* translated ^{35}S-labeled HIV-1 Vpu protein. The amount of Vpu bound was analyzed by SDS−PAGE and autoradiography. The experiment was repeated at least three times, and a representative set is shown. (B) Equivalent amounts of purified proteins (GST (lane 1), GST-SGT-TPR (lane 2), and GST-SGT (lane 3)) were analyzed by SDS−PAGE followed by Coomassie blue staining to ascertain the purity of the proteins.

Figure 2A, *in vitro* translated Vpu protein binds specifically to both GST-SGT (lane 3) and GST-SGT-TPR (lane 2) but not to GST alone (lane 1).

In order to determine the purity of the proteins, ~10 μg of GST (lane 1) and GST fusion proteins (lanes 2 and 3) were also separated on SDS−PAGE and subjected to Coomassie blue staining (Figure 2B). While the GST fusion form of SGT-TPR migrated as a single protein of the expected molecular mass (Figure 2B, lane 2), the GST fusion form of full-length SGT migrated at two molecular masses (Figure 2B, lane 3). The more intense band has the predicted molecular mass while the one that migrates faster probably corresponds to a degraded SGT product. This may be similar to the degradation product observed when the *Caenorhabditis elegans* SGT was expressed in bacteria (*21*). Attempts to separate this degraded product from full-length SGT by chromatography were unsuccessful (data not shown).

The TPR Domain of SGT Is Sufficient for the Inhibition of HIV-1 p24 Release. Previous studies showed that a high-level expression of hSGT in cells transfected with a HIV-1 proviral construct reduces the efficiency of viral particle release (*2*). Here, we cotransfected pXJ40flag-SGT or pXJ40flag-SGT-TPR with a HIV-1 proviral construct, pNL4-3.Luc.R-E- (*32, 33*), into 293T cells and determined the amount of HIV-1 p24, which is the viral capsid, secreted into the culture supernatant. Consistently, the overexpression of full-length SGT inhibits p24 release efficiently as the amount of p24 in the culture supernatant was approximately 20% when compared to the cells transfected with an empty pXJ40flag vector (Figure 3A). In the cells overexpressing SGT-TPR, the amount of p24 in the culture supernatant was also significantly reduced to ~50%, suggesting that the TPR domain is sufficient for this inhibition effect (Figure 3A).

Gel filtration analysis (data not shown) of SGT-TPR shows that it exists as a monomer, which is consistent with previous

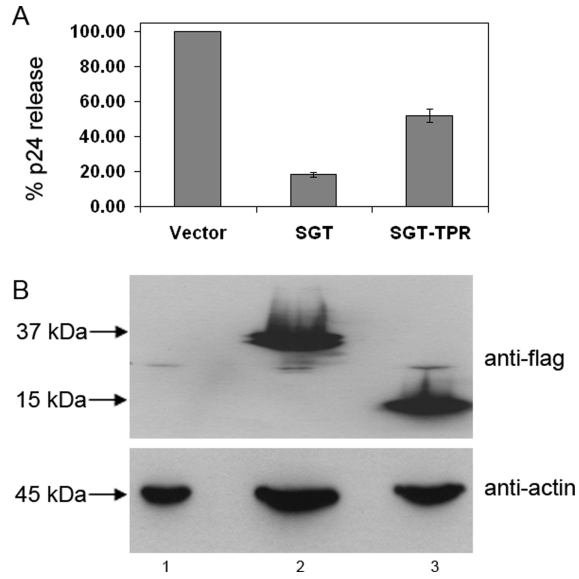

FIGURE 3: Effects of the overexpression of SGT on HIV-1 p24 release. (A) The amounts of HIV-1 secreted from cells cotransfected with pXJ40flag-vector, pXJ40flag-SGT, or pXJ40flag-SGT-TPR and a HIV-1 proviral construct were determined by measuring the amount of HIV-1 p24 capsid protein in the culture supernatant. The percentages of p24 release in the presence of full-length SGT or SGT-TPR were computed by normalizing the readings to the values for vector control (i.e., viral particle release in the presence of the pXJ40flag-vector is considered as 100%). All experiments were performed in triplicates, and the average values with standard deviations are plotted. The experiment was repeated at least three times, and a representative set is shown. (B) Total cell lysates were subjected to Western blot analysis to determine the expression of SGT (lane 2) or SGT-TPR (lane 3) (top panel). Lane 1 contained lysates from vector transfected cells. Equal amounts of lysates were used in each lane as verified by the level of endogenous actin (bottom panel).

findings that the N-terminus of hSGT is required for dimerization (*11*). In contrast, the barley SGT dimerizes via its TPR domain (*39*). Interestingly, the highly charged residues in the C-helix of barley SGT, which appear to be involved in the dimerization, are not conserved in the hSGT (*39*). Although we could not observe a significant difference between the binding of Vpu to SGT or SGT-TPR in the *in vitro* GST pull-down assay, it is possible that the dimerization of full-length SGT in the cellular compartment(s) leads to a more potent inhibition of Vpu-mediated virus release through additive effects.

Residues 31−35 in Vpu Are Important for Binding to SGT. To identify the SGT binding site in Vpu, a peptide array was designed from the protein sequence of Vpu. A total of 15 overlapping peptides were designed to cover the entire sequence of Vpu (MQPIIVAIVALVVAIIIAIVVWSIVI-IEYRKILRQRKIDRLIDRLIERAEDSGNESEGEVSALVE-MGVEMGHHAPWDIDDL). Peptides were immobilized onto a cellulose membrane and screened with SGT-TPR. Binding was detected with three overlapping peptides (Figure 4A). Similar results were obtained when the membrane was stripped and rescreened with SGT (data not shown). Residues 31−35 in Vpu (KILRQ) are found in three peptides that could bind SGT-TPR, suggesting that these residues are important for the interaction between Vpu and SGT. A fragment of Vpu, that contained residues 27−45, was expressed as a GST fusion protein (Figure 4B, upper panel), and GST pull-down assay was performed to confirm this

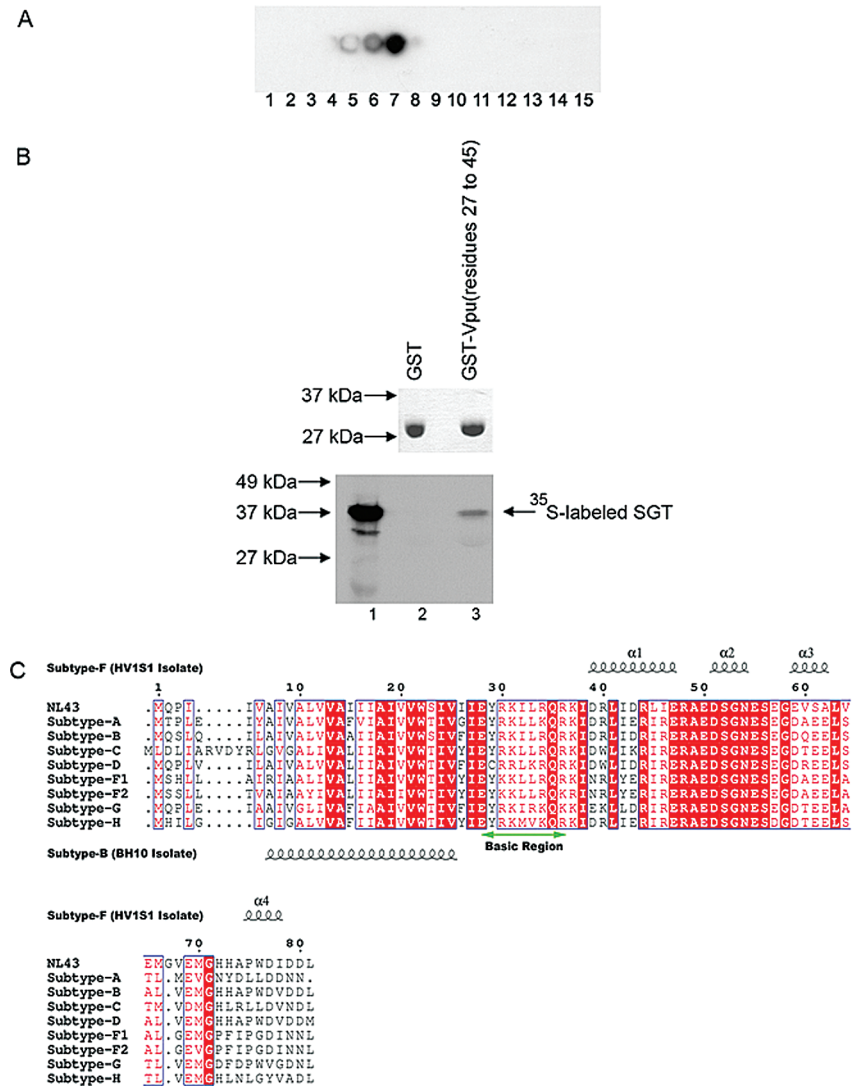

FIGURE 4: Identification of the SGT binding site in Vpu. (A) Overlapping peptides spanning the entire sequence of Vpu (81 amino acids) were designed so that each peptide consisted of 15 amino acids with an overlap of 10 amino acids. A total of 15 peptides were synthesized (1−15), immobilized onto a cellulose membrane, and screened with GST-SGT-TPR. Binding was detected with peptides 5 (VWSIVIIEYRKILRQ), 6 (IIEYRKILRQRKIDR), and 7 (KILRQRKIDRLIDRL), suggesting that the KILRQ motif in Vpu is important for binding to SGT. (B) GST (lane 2) and GST-Vpu (residues 27−45) (lane 3) were expressed in *E. coli*, affinity purified with glutathione−Sepharose beads, and analyzed by SDS−PAGE followed by Coomassie blue staining to ascertain the purity of the proteins (upper panel). GST pull-down assays were then carried out by mixing the bacterially expressed proteins bound to glutathione−Sepharose beads with *in vitro* translated ^{35}S-labeled SGT protein. The amount of Vpu bound was analyzed by SDS−PAGE and autoradiography (lower panel). One-tenth of the input was loaded in lane 1. (C) Vpu of the pNL4-3 clone used in this study is aligned with those of different HIV-1 M group subtypes. The consensus sequences for these subtypes (A, B, C, D, F1, F2, G, and H) were obtained from http://www.hiv.lanl.gov/. The structures of the transmembrane (residues 2−30) and cytoplasmic domains (residues 39−81) of Vpu have been solved independently by Park et al. (*58*) and Wilbold et al. (*46*), respectively. The positions of the α-helices in these domains are shown at the top and bottom. The basic region (marked with a green arrow), which is located between the transmembrane and cytoplasmic domains, is well conserved among all of the subtypes.

novel finding. As shown in Figure 4B, *in vitro* translated SGT protein binds specifically to GST-Vpu (residues 27−45) (lower panel, lane 3) but not to GST alone (lower panel, lane 2). Alignment of Vpu of the pNL4-3 clone with those of different HIV-1 M group subtypes revealed that the SGT binding site in Vpu is well conserved (Figure 4C).

DISCUSSION

SGT belongs to a family of cochaperones that interacts with both Hsp70 and Hsp90 via the so-called TPR domain, which consists of 34 amino acid motifs in tandem. In this study, we obtained a high-resolution three-dimensional structure of the TPR domain of SGT and showed that this domain adopts a compact and globular structure. This is consistent with a recent study which showed the TPR domain of SGT can fold cooperatively as an independent unit (*40*). The structure of SGT-TPR contains many typical features found in the structures of other TPR domains, and the highest degree of similarity is observed with the TPR domain of CHIP (*38*).

The TPR domains of several proteins, including SGT-TPR, have been shown to interact with the conserved EEVD motif found in the C-terminus of molecular chaperones Hsp70 and Hsp90 (*41*−*45*). Two well-studied Hsp70/Hsp90 binding proteins are CHIP and Hop (Hsp70/90 organizing protein). CHIP has been shown to bind either Hsp70 or Hsp90 through

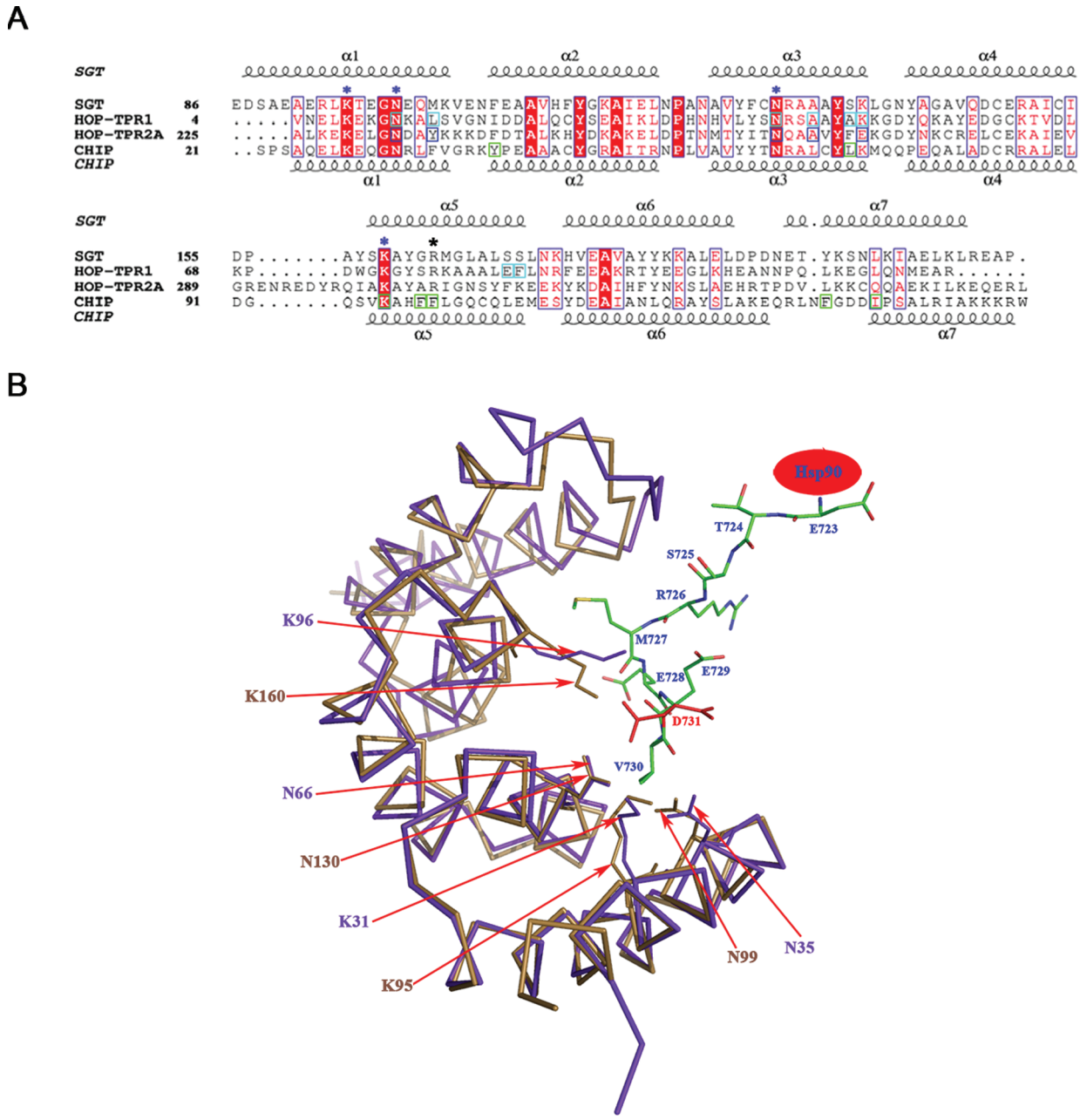

FIGURE 5: Structural comparison of the Hsp70/Hsp90 binding site in hSGT and CHIP. (A) Structural-based sequence alignment of hSGT, Hop, and CHIP TPR domains. Key residues involved in forming the carboxylate clamp are marked by blue stars. The black star represents an arginine conserved in most of the currently known Hsp70/Hsp90-binding TPR proteins except CHIP. Cyan, blue, and green boxes represent those residues in Hop TPR1, Hop TPR2A, and CHIP, respectively, that interact with residues upstream of the EEVD motif. (B) The TPR domain of hSGT is superimposed onto the CHIP TPR domain bound with the Hsp90 C-terminal decapeptide. The TPR domains of CHIP (deep purple) and hSGT (light brown) show high similarity, suggesting the mechanism of binding to Hsp70 or Hsp90 may be similar. The side chains of the key residues involved in forming the so-called carboxylate clamp are shown.

the same TPR domain whereas Hop utilizes two different TPR domains to bind Hsp70 and Hsp90 selectively. The high-resolution crystal structures of CHIP and Hop in complex with peptides containing the EEVD motif reveal that key residues involved in binding Hsp70/Hsp90 are conserved (*36, 38*). In CHIP, the side chains of Lys31, Asn35, Asn66, and Lys96 of the TPR domain make electrostatic interactions with the main chain and side chain of the C-terminal Asp731 of the Hsp90 peptide, whereas in Hop, equivalent residues Lys229, Asn233, Asn264, and Lys301 of the TPR2A domain make similar electrostatic interactions. With the Hop TPR1 domain, residues Lys8, Asn12, Asn43, Lys73, and Arg77 make electrostatic interactions with the C-terminal Asp641 of the Hsp70 peptide and align well with equivalent residues in both CHIP and Hop TPR2A (Figure 5A) (*36*). These electrostatic interactions are crucial to the formation of the so-called carboxylate clamp (*11, 20, 21, 24*).

SGT-TPR superimposes for the entirety with CHIP, Hop TPR1, and Hop TPR2A with rmsd of 0.94, 1.17, and 2.11 Å, respectively, reflecting similarity of these domains (Figure 5A). The highest degree of similarity is observed with CHIP where the Cα of the conserved side chains of Lys95, Asn99, Asn130, and Lys160 superimpose with rmsd of 0.57, 0.74, 0.21, and 0.60 Å, respectively, suggesting SGT-TPR most likely binds to the EEVD motif in Hsp70/Hsp90 with a

similar network of electrostatic interactions (Figure 5B). However, unique to CHIP, the side chain of Phe100 is involved in forming a hydrophobic pocket whereas the side chain of the equivalent residue in Hop TPR2A, Arg305, forms electrostatic interaction with Asp731 of Hsp90 and is conserved in all other TPR domains that bind Hsp70/Hsp90 (*36, 38*). The equivalent residue, Arg164, in SGT most likely contributes to forming the carboxylate clamp (Figure 5A).

Like CHIP, SGT can bind to both Hsp70/Hsp90 with similar affinities as demonstrated by Worrall et al. (*21*). Furthermore, in CHIP, a unique hydrophobic pocket is formed by side chains Lys96, Phe99, Phe100, Phe132, and IIe136, providing a binding site that can accommodate either Met727 of Hsp90 (DDTSRMEEVD) or IIe637 of Hsp70 (GSGPTIEEVD) (*38*). As a consequence, the bound peptide is twisted such that residues upstream of Met727 or IIe637 are pushed clear of the TPR domain and can no longer form additional contacts, explaining how CHIP can bind either Hsp70 or Hsp90 with similar affinities. However, with SGT-TPR, the residues involved in forming this hydrophobic pocket are absent, suggesting a different mechanism of dual recognition. In Hop, both TPR1 and TPR2A bind to the EEVD motif with a similar network of electrostatic interactions and as a consequence are not sufficient to account for the different specificity of TPR1 and TPR2A (*36*). Specificity is conferred by interactions with residues upstream of the EEVD motif. Crucial contacts between Hop TPR1 and Hsp70 involve hydrophobic interactions between Pro635 (Hsp70) and its binding cavity formed by Glu83 and Phe84 and van der Waals interaction between IIe637 (Hsp70) and Ala46, Ala49, and Lys50 (*36*). In TPR2A, Met727 (Hsp90) is involved in forming hydrophobic contacts with a cavity mainly formed by side chains Tyr236 and Glu271. Selectivity appears to be due to residues N-terminal to the EEVD motif binding to different hydrophobic pockets in TPR1 and TPR2A. In comparison with SGT-TPR, the only conserved residues in the Hsp70 binding region are equivalent to Ala46 and Lys50 in Hop TPR1. Whether these residues contribute to forming a binding pocket for Hsp70/Hsp90 in SGT and are responsible for dual recognition is unclear and requires further study.

Previous studies showed that full-length SGT can bind to both Vpu and Gag of HIV-1 (*2*), but SGT and Gag form a strong complex only in the absence of Vpu. Given that all three proteins are normally present in HIV-1 infected cells, we focused our investigations on the interaction between SGT and Vpu. It has also been demonstrated that the overexpression of hSGT in cells reduces the efficiency of HIV-1 particle release (*2*); however, the mechanism of inhibition is unclear, and it is not known if the TPR domain of SGT is required for this effect. In this study, we show that SGT-TPR can bind Vpu and reduce the amount of HIV-1 p24 secreted from cells transfected with the HIV-1 proviral construct. This indicates that SGT-TPR can inhibit the HIV-1 particle release, albeit at a lower efficiency than full-length SGT. Thus, the TPR domain of SGT is sufficient for the inhibition of HIV-1 particle release but the N- and/or C-terminus should also have some contributions. We also cannot rule out that the interaction between SGT and Gag is another important determinant for viral release especially since the expression of Vpu appears to cause the cellular localization of SGT and Gag to overlap (*10*). As it has not yet been determined which domain of SGT is involved in the interaction with Gag, it is possible that the N- and/or C-terminus of SGT also participate(s) in this interaction.

Unlike Hsp70 and Hsp90, Vpu does not contain any EEVD motif, suggesting that Vpu uses a different binding mechanism for its interaction with SGT. Using overlapping peptides and GST pull-down assay, we have identified five residues (^{31}KILRQ^{35}) in Vpu that are important for binding SGT. These residues are part of the so-called short basic region which is located between the transmembrane and cytoplasmic regions (*46*). The transmembrane and cytoplamic regions have been reported to be important for two separate functions of Vpu, with the former responsible for its ability to enhance viral release and the latter for its ability to downregulate the CD4 receptor (*47*−*49*). However, the role of the short basic region is unclear. This region appears to be highly flexible (*50, 51*), but some of the residues may be involved in salt bridge formations between the transmembrane helix and the first helix of the cytoplasmic domain (*52, 53*). By binding to the basic region, overexpressed SGT may interfere with the integrity of these salt bridges and/or create steric hindrance, thus reducing the ability of Vpu to anchor to the phosphoilpid bilayer via its transmembrane. Consequently, the ability of Vpu to mediate viral release is affected by the overexpression of SGT.

To our knowledge, there are three other TPR-containing cellular proteins that interact with viral proteins. The first one is the hepatitis B virus X-associated protein 2, XAP2, which was first identified by its ability to bind the hepatitis B virus X-protein (*54*). XAP2 contains a TPR domain at its C-terminus which is required for its interaction with Hsp90 (*55*). The second one is called rotavirus X protein associated with NSP3, RoXaN, which was first identified by its ability to bind the viral nonstructural protein NSP3 of rotavirus (*56*). RoXaN contains four TPR repeats at its N-terminus, but this region is not essential for its interaction with NSP3 (*56*). Lastly, the N-terminal TPR domain of the kinesin light chain (KLC) interacts with the cytoplamic tail of the viral protein A36R of vaccinia virus (*57*). Currently, there is no information on the three-dimensional structures of any of these virus-interacting TPR proteins.

In future studies, it will be crucial to determine if Vpu, SGT, and Hsp70/ Hsp90 can form ternary complexes and if these complexes are important for HIV-1 particle release. As our results suggest that the modes of binding for Vpu and Hsp70/Hsp90 to SGT are different, crystallization of these complexes is actively being pursued. Besides the viral proteins of HIV-1, SGT can also interact with the nonstructural protein of parvovirus H-1 (*1*) and the accessory protein ORF7a of the severe acute respiratory syndrome coronavirus (SARS-CoV) (*34*). However, the effects of SGT on the replication of parvovirus and SARS-CoV remain to be determined. The high-resolution three-dimensional structure of SGT-TPR provides a basis for future studies to define the precise roles of SGT in viral infections.

ACKNOWLEDGMENT

We thank Drs. Robinson and Song for sharing of equipment and Ms. Puay Yoke Tham and Daphne Chan and for technical assistance. The following reagent was obtained through the NIH AIDS Research and Reference Reagent

Program, Division of AIDS, NIAID, NIH: pNL4-3.Luc.R-E- from Dr. Nathaniel Landau.

REFERENCES

1. Cziepluch, C., Kordes, E., Poirey, R., Grewenig, A., Rommelaere, J., and Jauniaux, J. C. (1998) Identification of a novel cellular TPR-containing protein, SGT, that interacts with the nonstructural protein NS1 of parvovirus H-1. *J. Virol. 72*, 4149–4156.
2. Callahan, M. A., Handley, M. A., Lee, Y. H., Talbot, K. J., Harper, J. W., and Panganiban, A. T. (1998) Functional interaction of human immunodeficiency virus type 1 Vpu and Gag with a novel member of the tetratricopeptide repeat protein family. *J. Virol. 72*, 8461.
3. Maldarelli, F., Chen, M. Y., Willey, R. L., and Strebel, K. (1993) Human immunodeficiency virus type 1 Vpu protein is an oligomeric type I integral membrane protein. *J. Virol. 67*, 5056–5061.
4. Strebel, K., Klimkait, T., Maldarelli, F., and Martin, M. A. (1989) Molecular and biochemical analyses of human immunodeficiency virus type 1 vpu protein. *J. Virol. 63*, 3784–3791.
5. Willey, R. L., Maldarelli, F., Martin, M. A., and Strebel, K. (1992) Human immunodeficiency virus type 1 Vpu protein induces rapid degradation of CD4. *J. Virol. 66*, 7193–7200.
6. Chen, M. Y., Maldarelli, F., Karczewski, M. K., Willey, R. L., and Strebel, K. (1993) Human immunodeficiency virus type 1 Vpu protein induces degradation of CD4 in vitro: the cytoplasmic domain of CD4 contributes to Vpu sensitivity. *J. Virol. 67*, 3877–3884.
7. Strebel, K., Klimkait, T., and Martin, M. A. (1988) A novel gene of HIV-1, vpu, and its 16-kilodalton product. *Science 241*, 1221–1223.
8. Scarlata, S., and Carter, C. (2003) Role of HIV-1 Gag domains in viral assembly. *Biochim. Biophys. Acta 1614*, 62–72.
9. Bukrinskaya, A. G. (2004) HIV-1 assembly and maturation. *Arch. Virol. 149*, 1067–1082.
10. Handley, M. A., Paddock, S., Dall, A., and Panganiban, A. T. (2001) Association of Vpu-binding protein with microtubules and Vpu-dependent redistribution of HIV-1 Gag protein. *Virology 291*, 198–207.
11. Liou, S. T., and Wang, C. (2005) Small glutamine-rich tetratricopeptide repeat-containing protein is composed of three structural units with distinct functions. *Arch. Biochem. Biophys. 435*, 253–263.
12. Blatch, G. L., and Lassle, M. (1999) The tetratricopeptide repeat: a structural motif mediating protein-protein interactions. *BioEssays 21*, 932–939.
13. D'Andrea, L. D., and Regan, L. (2003) TPR proteins: the versatile helix. *Trends Biochem. Sci. 28*, 655–662.
14. Lamb, J. R., Tugendreich, S., and Hieter, P. (1995) Tetratrico peptide repeat interactions: to TPR or not to TPR? *Trends Biochem. Sci. 20*, 257–259.
15. Buchanan, G., Ricciardelli, C., Harris, J. M., Prescott, J., Yu, Z. C., Jia, L., Butler, L. M., Marshall, V. R., Scher, H. I., Gerald, W. L., Coetzee, G. A., and Tilley, W. D. (2007) Control of androgen receptor signaling in prostate cancer by the cochaperone small glutamine rich tetratricopeptide repeat containing protein alpha. *Cancer Res. 67*, 10087–10096.
16. Wang, H., Shen, H., Wang, Y., Li, Z., Yin, H., Zong, H., Jiang, J., and Gu, J. (2005) Overexpression of small glutamine-rich TPR-containing protein promotes apoptosis in 7721 cells. *FEBS Lett. 579*, 1279–1284.
17. Winnefeld, M., Grewenig, A., Schnolzer, M., Spring, H., Knoch, T. A., Gan, E. C., Rommelaere, J., and Cziepluch, C. (2006) Human SGT interacts with Bag-6/Bat-3/Scythe and cells with reduced levels of either protein display persistence of few misaligned chromosomes and mitotic arrest. *Exp. Cell Res. 312*, 2500–2514.
18. Winnefeld, M., Rommelaere, J., and Cziepluch, C. (2004) The human small glutamine-rich TPR-containing protein is required for progress through cell division. *Exp. Cell Res. 293*, 43–57.
19. Yin, H., Wang, H., Zong, H., Chen, X., Wang, Y., Yun, X., Wu, Y., Wang, J., and Gu, J. (2006) SGT, a Hsp90beta binding partner, is accumulated in the nucleus during cell apoptosis. *Biochem. Biophys. Res. Commun. 343*, 1153–1158.
20. Liu, F. H., Wu, S. J., Hu, S. M., Hsiao, C. D., and Wang, C. (1999) Specific interaction of the 70-kDa heat shock cognate protein with the tetratricopeptide repeats. *J. Biol. Chem. 274*, 34425–34432.
21. Worrall, L. J., Wear, M. A., Page, A. P., and Walkinshaw, M. D. (2007) Cloning, purification and characterization of the Caenorhabditis elegans small glutamine-rich tetratricopeptide repeat-containing protein, Biochim. Biophys. Acta.
22. Tobaben, S., Thakur, P., Fernandez-Chacon, R., Sudhof, T. C., Rettig, J., and Stahl, B. (2001) A trimeric protein complex functions as a synaptic chaperone machine. *Neuron 31*, 987–999.
23. Schantl, J. A., Roza, M., De Jong, A. P., and Strous, G. J. (2003) Small glutamine-rich tetratricopeptide repeat-containing protein (SGT) interacts with the ubiquitin-dependent endocytosis (UbE) motif of the growth hormone receptor. *Biochem. J. 373*, 855–863.
24. Angeletti, P. C., Walker, D., and Panganiban, A. T. (2002) Small glutamine-rich protein/viral protein U-binding protein is a novel cochaperone that affects heat shock protein 70 activity. *Cell Stress Chaperones 7*, 258–268.
25. Rost, B., Yachdav, G., and Liu, J. (2004) The PredictProtein server. *Nucleic Acids Res. 32*, W321–W326.
26. Otwinowski, Z., and Minor, W. (1997) Processing of X-ray diffraction data collected in oscillation mode. *Methods Enzymol. 276*, 307–326.
27. Yang, J., Roe, S. M., Cliff, M. J., Williams, M. A., Ladbury, J. E., Cohen, P. T., and Barford, D. (2005) Molecular basis for TPR domain-mediated regulation of protein phosphatase 5. *EMBO J. 24*, 1–10.
28. Collaborative Computational Project, No. (1994) The CCP4 Suite: Programs for Protein Crystallography. *Acta Crystallogr. D 50*, 760.
29. Brunger, A. T., Adams, P. D., and Rice, L. M. (1998) Recent developments for the efficient crystallographic refinement of macromolecular structures. *Curr. Opin. Struct. Biol. 8*, 606–611.
30. Jones, T. A., Zou, J. Y., Cowan, S. W., and Kjeldgaard, M. (1991) Improved methods for building protein models in electron density maps and the location of errors in these models. *Acta Crystallogr. A 47*, 110–119.
31. Laskowski, R., MacArthur, M., Moss, D., and Thornton, J. (1993) PROCHECK: A program to check the stereochemical quality of protein structures. *J. Appl. Crystallogr. 26*, 283–291.
32. Connor, R. I., Chen, B. K., Choe, S., and Landau, N. R. (1995) Vpr is required for efficient replication of human immunodeficiency virus type-1 in mononuclear phagocytes. *Virology 206*, 935–944.
33. He, J., Choe, S., Walker, R., Di Marzio, P., Morgan, D. O., and Landau, N. R. (1995) Human immunodeficiency virus type 1 viral protein R (Vpr) arrests cells in the G2 phase of the cell cycle by inhibiting p34cdc2 activity. *J. Virol. 69*, 6705–6711.
34. Fielding, B. C., Gunalan, V., Tan, T. H., Chou, C. F., Shen, S., Khan, S., Lim, S. G., Hong, W., and Tan, Y. J. (2006) Severe acute respiratory syndrome coronavirus protein 7a interacts with hSGT. *Biochem. Biophys. Res. Commun. 343*, 1201–1208.
35. Tan, Y. J., Teng, E., Shen, S., Tan, T. H., Goh, P. Y., Fielding, B. C., Ooi, E. E., Tan, H. C., Lim, S. G., and Hong, W. (2004) A novel severe acute respiratory syndrome coronavirus protein, U274, is transported to the cell surface and undergoes endocytosis. *J. Virol. 78*, 6723–6734.
36. Scheufler, C., Brinker, A., Bourenkov, G., Pegoraro, S., Moroder, L., Bartunik, H., Hartl, F. U., and Moarefi, I. (2000) Structure of TPR domain-peptide complexes: critical elements in the assembly of the Hsp70-Hsp90 multichaperone machine. *Cell 101*, 199–210.
37. Grizot, S., Fieschi, F., Dagher, M. C., and Pebay-Peyroula, E. (2001) The active N-terminal region of p67phox. Structure at 1.8 Å resolution and biochemical characterizations of the A128V mutant implicated in chronic granulomatous disease. *J. Biol. Chem. 276*, 21627–21631.
38. Zhang, M., Windheim, M., Roe, S. M., Peggie, M., Cohen, P., Prodromou, C., and Pearl, L. H. (2005) Chaperoned ubiquitylation-crystal structures of the CHIP U box E3 ubiquitin ligase and a CHIP-Ubc13-Uev1a complex. *Mol. Cell 20*, 525–538.
39. Nyarko, A., Mosbahi, K., Rowe, A. J., Leech, A., Boter, M., Shirasu, K., and Kleanthous, C. (2007) TPR-Mediated self-association of plant SGT1. *Biochemistry 46*, 11331–11341.
40. Cortajarena, A. L., and Regan, L. (2006) Ligand binding by TPR domains. *Protein Sci. 15*, 1193–1198.
41. Ballinger, C. A., Connell, P., Wu, Y., Hu, Z., Thompson, L. J., Yin, L. Y., and Patterson, C. (1999) Identification of CHIP, a novel tetratricopeptide repeat-containing protein that interacts with heat shock proteins and negatively regulates chaperone functions. *Mol. Cell. Biol. 19*, 4535–4545.
42. Bell, D. R., and Poland, A. (2000) Binding of aryl hydrocarbon receptor (AhR) to AhR-interacting protein. The role of hsp90. *J. Biol. Chem. 275*, 36407–36414.
43. Carrello, A., Allan, R. K., Morgan, S. L., Owen, B. A., Mok, D., Ward, B. K., Minchin, R. F., Toft, D. O., and Ratajczak, T. (2004)

Interaction of the Hsp90 cochaperone cyclophilin 40 with Hsc70. *Cell Stress Chaperones 9*, 167–181.
44. Chen, S., and Smith, D. F. (1998) Hop as an adaptor in the heat shock protein 70 (Hsp70) and hsp90 chaperone machinery. *J. Biol. Chem. 273*, 35194–35200.
45. Young, J. C., Hoogenraad, N. J., and Hartl, F. U. (2003) Molecular chaperones Hsp90 and Hsp70 deliver preproteins to the mitochondrial import receptor Tom70. *Cell 112*, 41–50.
46. Willbold, D., Hoffmann, S., and Rosch, P. (1997) Secondary structure and tertiary fold of the human immunodeficiency virus protein U (Vpu) cytoplasmic domain in solution. *Eur. J. Biochem. 245*, 581–588.
47. Bour, S., and Strebel, K. (2003) The HIV-1 Vpu protein: a multifunctional enhancer of viral particle release. *Microbes Infect. 5*, 1029–1039.
48. Montal, M. (2003) Structure-function correlates of Vpu, a membrane protein of HIV-1. *FEBS Lett. 552*, 47–53.
49. Hout, D. R., Mulcahy, E. R., Pacyniak, E., Gomez, L. M., Gomez, M. L., and Stephens, E. B. (2004) Vpu: a multifunctional protein that enhances the pathogenesis of human immunodeficiency virus type 1. *Curr. HIV Res. 2*, 255–270.
50. Federau, T., Schubert, U., Flossdorf, J., Henklein, P., Schomburg, D., and Wray, V. (1996) Solution structure of the cytoplasmic domain of the human immunodeficiency virus type 1 encoded virus protein U (Vpu). *Int. J. Pept. Protein Res. 47*, 297–310.
51. Wray, V., Kinder, R., Federau, T., Henklein, P., Bechinger, B., and Schubert, U. (1999) Solution structure and orientation of the transmembrane anchor domain of the HIV-1-encoded virus protein U by high-resolution and solid-state NMR spectroscopy. *Biochemistry 38*, 5272–5282.
52. Fischer, W. B. (2003) Vpu from HIV-1 on an atomic scale: experiments and computer simulations. *FEBS Lett. 552*, 39–46.
53. Sramala, I., Lemaitre, V., Faraldo-Gomez, J. D., Vincent, S., Watts, A., and Fischer, W. B. (2003) Molecular dynamics simulations on the first two helices of Vpu from HIV-1. *Biophys. J. 84*, 3276–3284.
54. Kuzhandaivelu, N., Cong, Y. S., Inouye, C., Yang, W. M., and Seto, E. (1996) XAP2, a novel hepatitis B virus X-associated protein that inhibits X transactivation. *Nucleic Acids Res. 24*, 4741–4750.
55. Meyer, B. K., and Perdew, G. H. (1999) Characterization of the AhR-hsp90-XAP2 core complex and the role of the immunophilin-related protein XAP2 in AhR stabilization. *Biochemistry 38*, 8907–8917.
56. Vitour, D., Lindenbaum, P., Vende, P., Becker, M. M., and Poncet, D. (2004) RoXaN, a novel cellular protein containing TPR, LD, and zinc finger motifs, forms a ternary complex with eukaryotic initiation factor 4G and rotavirus NSP3. *J. Virol. 78*, 3851–3862.
57. Ward, B. M., and Moss, B. (2004) Vaccinia virus A36R membrane protein provides a direct link between intracellular enveloped virions and the microtubule motor kinesin. *J. Virol. 78*, 2486–2493.
58. Park, S. H., De Angelis, A. A., Nevzorov, A. A., Wu, C. H., and Opella, S. J. (2006) Three-dimensional structure of the transmembrane domain of Vpu from HIV-1 in aligned phospholipid bicelles. *Biophys. J. 91*, 3032–3042.

BI800758A